Photocatalytic reactors for Environmental Remediation: A review.

Cathy McCullagh, Nathan Skillen, Morgan Adams and Peter K.J. Robertson*

IDeaS, Innovation, Design and Sustainability Research Institute, Robert Gordon University, Schoolhill, Aberdeen, AB10 1FR, UK

*Corresponding Author:

Tel: +44 1224 263750

Fax: +44 1224 262759

peter.robertson@rgu.ac.uk

Abstract

OVERVIEW

Research in the field of photocatalytic reactors in the past three decades has been an area of extensive and diverse activity with an extensive range of suspended and fixed film photocatalyst configurations being reported. The key considerations for photocatalytic reactors, however, remain the same; effective mass transfer of pollutants to the photocatalyst surface and effective deployments and illumination of the photocatalyst.

IMPACT

Photocatalytic reactors have the potential versatility to be applied to the remediation of a range of water and gaseous effluents. Furthermore they have also been applied to the treatment of potable waters.

APPLICATIONS

Photocatalytic reactors are being scaled-up for consideration within waste and potable water treatment plants. Furthermore systems for the reduction of carbon dioxide to fuel products have also been reported.

Keywords: Photocatalyst, reactor, fluidised bed, immobilised film, suspended catalyst mass transport, rate control.

INTRODUCTION

The application of semiconductor photocatalysis in the fields of engineering and science is an important area of research which has grown significantly in the last three decades with increasing numbers of publications appearing every year [1-6]. Semiconductor photocatalysis has been applied to a diverse array of environmental problems including air, potable and wastewater treatment. This versatile process has also been utilised for the destruction of micro-organisms such as bacteria[6, 7], viruses [8] and for the inactivation of cancer cells[9, 10]. Semiconductor photocatalysis has also been applied to the photo-splitting of water to produce hydrogen gas [11-14], nitrogen fixation [15-18] and for the remediation of oil spills [19-21].

Heterogeneous photocatalysis for the remediation of polluted water streams falls into two distinct areas. Firstly the focus is on basic chemical transformations on semiconductor photocatalyst materials. These investigations have concentrated on the examination of basic photocatalytic processes such as including photocatalytic material science, surface interactions on photocatalysts, reaction mechanisms and kinetics that impact on the processes on a molecular level [1-5].

In order to demonstrate the viability of semiconductor photocatalysis for environmental remediation, reactor design is an equally critical factor. Effective reactor design research and development aims to scale up lab bench scale processes to industrially feasible applications. Scaling up photocatalytic reactors is, however a complex process with many factors needing consideration to yield a technically and economically efficient process. These factors include distribution of pollutant and photocatalyst, pollutant mass transfer, reaction

kinetics and irradiation characteristics. The issue of effective photocatalyst illumination is particularly important as this essentially determines the amount of water that may be treated per effective unit area of deployed photocatalyst. A wide range of photocatalytic reactors have been developed and used in both basic research and pilot scale studies. The central problem of scale-up of photocatalytic reactors is the provision of sufficient high specific surface area of catalyst and the uniform distribution of illumination across this area.

Mechanism of heterogeneous photocatalysis

As a process for water purification, photocatalysis has vast advantages over many existing technologies. The technique can result in the mineralisation of pollutants rather than transferring them to an alternative phase, such as is the case with activated carbon adsorption. Furthermore photocatalysis does not require the use of hazardous materials such as hypochlorite, peroxide or ozone[4]. Titanium dioxide is the catalyst of choice as it is inexpensive, non-toxic, chemically stable and is highly photocatalytically active[2]. TiO_2 acts as a photocatalyst due to its electronic structure, characterised by an electronically filled valence band and empty conduction band[22] separated by a band gap. If a photon of energy greater than or equal to the bandgap energy, E_g, is absorbed by TiO_2, an electron is promoted from the valence band to the conduction band. This generates a reducing electron in the conductance band and an oxidising hole in the valence band (figure 1). The excited conduction band electrons may recombine with the valence band holes generating heat energy. Alternatively they may be trapped in surface states, undergo reactions with electron donating or accepting species that are adsorbed on the TiO_2 surface. The electron and

holes formed are highly charged and result in redox reactions, which can ultimately result in the mineralisation of aqueous pollutants. Hydroxyl radicals are believed to be generated on the surface of TiO_2 through a reaction of the valence band holes with adsorbed water, hydroxide or surface titanol groups (Eq 2). The photogenerated conductance band electrons react with electron acceptors such as oxygen which generates superoxide (O_2^-) (Eq 4). Thermodynamically the redox potential of the TiO_2 electron/hole pair should enable the production of hydrogen peroxide, primarily via the reduction of adsorbed oxygen[3, 23, 24](Eqn 1-7).

$$TiO_2 + h\nu \rightarrow TiO_2(e^-_{cb} + h^+_{vb}) \quad (1)$$

$$h^+_{vb} + OH^-_{,ads} \rightarrow OH^\bullet_{,ads} \quad (2)$$

$$OH^\bullet_{,ads} + \text{Reactant} \rightarrow \text{Oxidised products} \quad (3)$$

$$e^-_{tr} + O_{2,ads} \rightarrow O_2^{\bullet -} \quad (4)$$

$$O_2^{\bullet -} + H^+ \rightarrow HO_2^\bullet \quad (5)$$

$$HO_2^\bullet + HO_2^\bullet \rightarrow H_2O_2 + O_2 \quad (6)$$

$$H_2O_2 + e^-_{cb} \rightarrow {}^\bullet OH + OH^- \quad (7)$$

Figure 1 illustrates the basic processes involved in photocatalysis.

Figure 1:

TYPES OF REACTOR CONFIGURATIONS

A wide variety of reactor configurations have been reported in the literature over the past 30 years including:

- annular photoreactor [25, 26],
- packed bed photoreactor [27],
- photocatalytic Taylor vortex reactor [28-31],
- fluidised bed reactor [32, 33],
- coated fibre optic cable reactor [34],
- falling film reactor [35],
- thin film fixed bed sloping plate reactor [36],
- swirl flow reactor [37],
- corrugated plate reactor [38].

Table 1 shows a comprehensive yet not exhaustive overview of photoreactor type, reactant phase, experimental targets, catalyst employed and industrial applications.

Table 1.

Examples of these various reactors will be considered in the following sections.

Suspended Liquid Reactors

Slurry / Suspension systems

TiO_2 catalysts have been investigated in both slurry/suspension systems and immobilised systems. The main advantage of using photocatalyst slurries is the larger surface area compared to the immobilised system. The separation of the

nanometre catalyst particles is, however, expensive and is a major drawback in the commercialisation of this type of system [39]. Nan Chong *et al.* [40] have reported the use of H-titanate nanofibres in an annular slurry photoreactor. They studied congo red as a model compound but one of the key advantages was the settling velocity of the catalyst. Using Kynch's theory batch settling trials revealed that the H-titanate nanofibre photocatalysts resulted in a settling velocity of 8.38 x 10^{-4}-4 m s^{-1}. The authors proposed that these novel nanoparticles could deliver a true engineering solution to catalyst separation on an industrial scale. It was also reported that it was difficult to effect irradiation of all the photocatalyst particles in the slurry in the unit due to shielding from the light source of the particles in the body of the unit form particles closer to the reactor walls.. Therefore depth of light penetration into the slurry reactor was restricted.

It has been reported the ratio between backward reflected and incident photon flow is strongly influenced by the geometry within the reactor. The Apparent Napierian Extinctance (ANE) coefficient for slurries is a parameter which is related to the photon absorption rate[41] . ANE depends on the particle size and is inversely proportional to the particle size where:

$$(ANE)_{\lambda} = - \ln (I/I_o) \qquad (8)$$

I is the outgoing light intensity after interaction with catalyst suspension and I_o represents the light intensity obtained in a blank setup. The absorption of light within slurry systems cannot be separated from scattering, which makes kinetic analysis of experiments more challenging [42].

An alternative approach is to attach the catalyst to a transparent stationary support over which the contaminated water passes. In such a system it is possible achieve effective illumination of all the photocatalyst deployed in the reactor [43, 44]. There are, however, also problems associated with immobilised systems which include the dependence on mass transfer of pollutant to the photocatalyst surface and the ensuring effective access to the photocatalyst surface of both activating photons and reacting molecules to the photocatalyst surface[45]. The photocatalyst film thickness may affect the internal mass transfer as it may not be possible to access the photocatalyst material in the proximity of the support-catalyst interface. Each of these factors will result in a reduction in the rates of decomposition in immobilised film photocatalyst units when compared to slurry processes.

An early slurry based reactor effected the complete mineralisation of chloroform to chloride and CO_2 [46]. This study was further supported by Kormann *et al* [47] who demonstrated the complete dehalogenation of chloroform but also illustrated an increase in $[Cl^-]$ as a function of time. Pramauro *et al.* [48] reported the complete degradation of monuron (figure 2a), a persistent herbicide, within one hours photocatalysis. The reaction conditions investigated were simulated solar irradiation, TiO_2 slurry and a batch reactor. Several intermediate products were determined after 30 minutes irradiation; these were not detected at the end of the irradiation time. The complete degradation and dechlorination of 3,4-dichloropropionamide (figure 2b), another persistent herbicide was reported by Pathirana and Maithreepala [49] using a TiO_2 suspension photocatalytic reactor. It was reported that the dechlorination of the herbicide was dependent on TiO_2

concentration, and higher photocatalyst levels caused TiO_2 a shielding effect of the incident light. Li Puma and Yue [50] investigated the kinetics of degradation of single component and multi-component systems of chlorophenols. They studied the simultaneous use of short, medium and long wavelength ultra-violet light to investigate the integration of simultaneous photocatalysis and photolysis. The optimal loading of photocatalyst for the geometry of their batch reactor via the oxidation of 2-CP to CO_2 was determined as part of this investigation with mineralization rates achieving a 3-fold increase up to a maximum photocatalyst loading of 0.5 mg L^{-1}. In the single component experiments the kinetics were too complex to allow the authors to determine whether the photolytic pathway would be preferential to the photocatalytic pathway or vice versa. During the multi-component experiments they observed that the overall oxidation kinetics were controlled by the reactant in excess, as the substrate present in smaller concentrations was found to degrade at a much slower rate than that in the single-component experiments. Overall the authors demonstrated that the entire course of photocatalytic oxidation of single-component and multi-component systems of chlorophenols can be predicted satisfactorily using simple kinetic models that could be useful in the design and modelling of large scale photocatalytic reactors. This work was followed by studies of a pilot-scale continuous-flow laminar falling film slurry photocatalytic reactor (LFFSIW)[51], which utilised commercially available UV lamps. A comprehensive investigation of this unit was reported looking at a range of parameters including; the wavelength and intensity of the incident irradiation source, the influence of additional oxidising reagents, the concentrations of both reactants and photocatalyst and the irradiation time. Li Puma and Yu also studied six different photon based processes, and determined that the UVC photocatalysis/UVC

photolysis/UVC peroxidation process was superior to UVA photocatalysis, UVC photocatalysis/UVC photolysis, UVA photocatalysis/UVA peroxidation, UVC photolysis/UVC peroxidation and UVC photolysis systems. The results of the experiments conducted at different incident radiation intensities clearly indicated that low-wattage UVC lamps were preferable to high-wattage UVC lamps because enhancements of reactor conversions due to higher lamp power were offset by an increase in electricity costs.

FIGURE 2

Further work by Li Puma and Yue [35] compared the effectiveness of a range of photooxidation processes in a falling film pilot reactor. They investigated UVA-photocatalysis, UVA-photocatalysis-peroxidation, UVC-photolysis, UVC-photolysis-peroxidation, UVC-photocatalysis-photolysis and UVC-photocatalysis-photolysis-peroxidation. They selected salicylic acid as a model compound for all experiments. The highest conversion of salicylic acid was 58%, which was obtained with the UVC-photolysis-peroxidation process. Conversely the highest conversion to CO_2 was obtained with the UVC-photocatalysis-photolysis-peroxidation process (28%) and the lowest value was with the UVA-photocatalysis process (1.7%). The mineralisation efficiency of the photocatalytic and the photolytic-photocatalytic processes was in the range 58-65%, far above that of the photolytic process which was in the range of 14-18%.

San *et al.* [52] investigated the photodegradation of 3-aminophenol (3-AP) in a TiO_2 batch suspension photoreactor. They reported that this process followed pseudo-first-order kinetics, with the apparent rate constant depending on the

initial 3-AP concentration. Furthermore the addition of electron acceptors enhanced the reaction rate significantly.

A study of the adsorption and photocatalytic degradation of the safira HEXL dye, has been reported using a TiO_2 slurry reactor[53]. The authors concluded that the dye adsorption to the photocatalyst surface was critical for the efficient photocatalytic degradation. The process was also pH dependent with an improved degradation rate observed near the point of zero charge of TiO_2. The slurry TiO_2 catalyst has also been employed within an internally circulating bubble column reactor for the degradation of trichloroethylene with a removal efficiency of 97% reported[54]. Employing a photocatalyst filtration with a bubble column reactor and TiO_2 slurry may be efficient process for the destruction of phenoxyacetic acid[55]. This overcomes one of the major drawbacks of slurry systems, separation of catalyst from remediated waste stream.

Adams *et al* [56] reported the comparison of a standard flat plate reactor with a novel drum reactor[57] for the removal of oil and gas hydrocarbon contaminants from water. The flat plate design was constructed from polymethylmethacrylate (PMMA) and was as a small scale lab unit, however, a 'concertina' designed reactor was proposed for the scale up. The drum reactor concept was a single pass continuous flow system for the treatment of waste water/effluents which utilised rotating paddles to ensure an even distribution of catalyst[56] (figure 3).

FIGURE 3

The reactor set up utilised three connecting drum reactors. The paddles positioned on the inside of the reactor drum were placed as to allow the removal of pellets from the reaction solution allowing for exposure to UV illumination before returning to the main stock[56, 57]. Dependant on the level of contaminant present the effluent would pass from one 'drum' to another for prolonged treatment. On average the sample would reside in each drum for approximately 3 min with the overall reaction time at approximately 10 min. In the event of the final sample still being of a high hydrocarbon concentration the effluent would be recirculated into the system. As an attempt to develop a reactor deemed more environmentally efficient, pelletised catalyst was used to reduce downstream processing restrictions associated with the filtration of powdered catalyst. While both designs proved effective in the removal of hydrocarbons the drum reactor achieved 90 % removal in less than 10 min. This high level of reduction over a short period of time is attributed to samples passing through the 3 consecutive drums each with 200 g of TiO_2 catalyst present, therefore utilising 600 g for the entire system. The flat plate design was investigated in regards to optimising conditions to provide maximum destruction. It was concluded that a lower angled plate increases retention times of compounds and thus a chance of successful catalyst-pollutant interface[56]. The addition of air and hydrogen peroxide to increase destruction proved effective with 80% degradation over 135 min recorded for H_2O_2 compared to 40 % for air alone.

In a subsequent paper McCullagh *et al.* [58] described the degradation of methylene blue (MB) in a slurry continuous flow drum reactor (figure 4). A 98 % degradation of MB over 60 min of illumination utilising a high loading weight of 30 g L^{-1} of TiO_2 pellets was reported. The investigation of different loading weights concluded that a maximum weight of 180 g of catalyst was attainable.

While 98% degradation was recorded for 30 g catalyst (Pellet form) over 60 min, the use of Degussa P25 as a photocatalyst was significantly more efficient with 90% of the MB be decomposed within 20 min photocatalysis.

FIGURE 4

Further evaluation of the drum reactor has been carried out in the remediation of oily waste water (OWW) from an interceptor tank[59]. This study showed the unit achieved a 50% reduction in abundance for both decane and dodecane after 90 min UV photocatalysis along with a >50 % abundance reduction in tetradecane. Following a further 90 min illumination period of the OWW in the reactor all volatile organic compounds (VOC) initially identified were almost completely removed. Additionally total organic carbon TOC was investigated showing a 35 % reduction in TOC for OWW samples passed twice through the reactor. The results highlighted demonstrate a high efficiency for a novel photocatalytic reactor with large scale applications as a polishing technique to be coupled with current water treatment processes [59].

Mass Transfer Limitations within TiO_2 slurry reactors

Mass transfer within slurry reactors has not received a great deal of attention primarily as such problems have not been recognised as being major impediments to the application of a slurry reactor. Chen and Ray [60] did not observe either intra or extra particle diffusive limitations when working with a suspended solid reactor. Considering the optical thickness of the suspension Martin *et al*.[61] found a loss in reactor efficiency when the optical thickness of the suspension was greater than an calculated optimum level. For large catalyst loading restrictions with mass and radiation transport inside the catalytic particle has been reported by Mehrotra *et al.* [62]. Peralta Muniz Moreira [63] found no

diffusion limitations within their reactor when pseudo 1st order kinetics were applied along with the Weiz and Prater criterion. How mass transport influences the rate of reaction within slurry reactors is very important in order to obtain relevant kinetic information about the reaction but also for photoreactor design. Ballari *et al.* [64] investigated the effects of photocatalyst irradiation, photocatalyst loadings, flow rates, total suspension volume and changes in illumination length of the reactor. They found significant concentration gradients that were likely to cause limitations in mass transport resulted from the non-uniformity of the irradiation area. The authors state that these concentration gradients are difficult to avoid but could be eradicated if a fully developed turbulent flow operated within the reactor. They concluded that mass transport problems could be overcome using a 1 g/L catalyst loading, irradiation rates of 1 x 10^{-7} Einsteins cm^{-1} s^{-1} and effective mixing.

Fluidised bed reactors

The application of fluidised bed reactors have been extensively reported with round 1000 published on this topic over the past 6 years [32, 64-74]. Fluidised bed reactors are capable of utilising an upward stream of fluid (gas or liquid) to allow particles in a stationary phase to be brought to a suspended or 'fluidised' state allowing for photocatalytic transformations to occur (figure 5).

FIGURE 5

The advantages of this style of reactors include:

- a low pressure drop,
- high throughput and

- high photocatalyst surface area which consecutively allows for increased catalyst-reactant interaction.

In 1992 Dibble and Raupp[66] used a flat plate fluidised bed reactor (figure 6) to photoxidise trichloroethylene (TCE). A quantum efficiency range of 2-13 % was achieved with a reaction rate peaking at 0.8µmol TCE (g of catalyst)$^{-1}$ min^{-1} [2 µmol/(g of TiO_2)$^{-1}$ min^{-1}]. These results are significant in that they are comparable to results produced in a liquid-solid slurry system for the oxidation of TCE, specifically demonstrating an order of magnitude increase. TCE is a standard evaluation test carried out by many including more recently Lim and Kim who investigated a circulated fluidised bed reactor (CFDB) [67]. The design of this reactor used a loop seal which allowed particles that were carried up by the air stream to flow back down and re-enter the system. Several other factors were investigated in this paper including UV wavelength, initial TCE concentration, circulation rate and O_2 and H_20 concentrations.

FIGURE 6

A two-dimensional fluidised bed reactor was used by Lim *et al.*[75] in order to decompose NO. Reported in the research was efficient contact between the catalyst (P-25) and reactant gas (NO) which, when coupled with good UV-light transmission allowed for increased NO decomposition in comparison to an annular flow-type photoreactor. A series of altering conditions were tested as a means to increase photocatalytic efficiency including; initial gas concentration, residence time of gas, reaction temperature and irradiation intensity. A particular point of interest in this publication surrounded the superficial gas velocity and light transmission interaction. Results displayed in figure 7 show

increasing superficial gas velocity increased light transmission with light intensity significantly increasing at approx. 1.3 U_{mf} (minimum fluidisation velocity) which equated to a sharp increase in NO conversion at 1.3 U_{mf}. Below this value the UV light was not capable of transmitting through the catalyst bed. An increasing trend is observed until the U_{mf} reaches 2.5, where a 70 % photocatalytic decomposition of NO was recorded. Conversion recorded after this point was regarded as a result of NO bypassing through bubbles and the reduction of gas residence time in the catalysts bed[69, 75]. Based upon their results Lim *et al.* [75] concluded that NO photocatalytic decomposition required adequate residence time and an effective NO gas velocity to enable the appropriate bubble size formation enabling appropriate contact between UV light and the TiO_2-NO system.

FIGURE 7

Son *et al.*[70] investigated the use of combined TiO_2 particles with Al_2O_3 in an attempt to overcome the drawbacks associated with fluidised reactors for photocatalysis. Paz [65] reported that fluidisation of small particles such as P-25 was challenging due to 'drifting' from the primary operation area in the unit. Combining the catalyst, however, with larger particles such as Al_2O_3 could eliminate this problem and as such many researchers use an Al-TiO_2 catalyst. Son [70] focused on the decomposition of acetic acid and ammonia utilising a three phase photocatalytic system. Decomposition during the research was enhanced when carried out in the three-phase fluidised bed reactor, showed significant improvement over use in a steady reactor. Production of N_2 and CO_2 were monitored as means of measuring acetic acid and ammonia decomposition. In terms of acetic acid decomposition the fluidised bed showed increased efficiency

over that of a conventional steady reactor along with increased efficiency by the addition of Al-TiO_2 instead of solely TiO_2; the conversion of acetic acid to CO_2 reached approximately 90 % after 600 min with 10 mol% Al-TiO_2. A similar trend was observed for ammonia decomposition with a conversion rate of >95 % being reached with 10 mol% Al-TiO_2 compared to that of 70 % in the steady reactor. A point of interest is the suppression of the more undesirable products of NO_2 and NO_3 with the use of Al-TiO_2 when compared to increased levels with pure TiO_2. In a previous study which used a $FeTiO_2$ material it was reported that the anatase structure of the catalyst transformed into a rutile structure after methanol destruction[71]. Son *et al.* [70], however, found replacing the Fe with Al produces a catalyst with increased stability, thus providing enhancing ammonia decomposition. They concluded from their results that the removal of VOC efficiency is increased by both the use of Al-TiO_2 combined particles and a fluidised reactor.

Nelson *et al.*[72] reported the comparison of a fluidised TiO_2 system for methanol oxidation with a packed bed reactor. They concluded that fluidisation resulted in faster rates of photocatalytic decomposition than achieved on the packed bed unit. A rate of 2.0 x 10^{-7} mol/cm^3 cat/min for CO_2 production was achieved for the fluidised reactor compared to a CO_2 production rate of 1.0 x10^{-7} mol/cm^3 cat/min obtained with the packed bed reactor. It was reported that the use of both static mixing and vibration in the process to reduce photocatalyst separation rates was, however, only effective with Degussa P25 and not TiO_2-Al_2O_3. Overall TiO_2-Al_2O_3 was found to be an effective photocatalyst which is in agreement with the results obtained by Paz [65].

The drawbacks to fluidising pure TiO_2 has led to an increased number of papers reporting results using combined catalyst, demonstrated by Kuo *et al.* [32] who investigated the removal of toluene vapours from a continuous gas stream. The specific limitations include the 'loss or trapping' of powder within a photoreactor due to the fine structure of TiO_2. These problems can often result in the powdered catalyst 'drifting' away from the main area of operation. The investigation used activated carbon (AC) particles with a TiO_2 coating to overcome any fluidisation problem and promote good evenly distributed catalyst. The research investigated the impact of altered relative humidity (RH), varied TiO_2 loading weights, and the use of glass beads (GB) in replacement of AC along with and without the use of a reflector. The use of activated carbon solely is effective in the removal of toluene, however, upon saturation of the AC particles toluene removal decreased significantly. It was established that 30% RH was optimal for efficient toluene removal. Interestingly increasing RH did not result in increased rates of toluene removal suggesting there is competitive adsorption between water and toluene molecules at higher levels of RH. The degradation of toluene vapours was accredited to both the use of activated carbon and photocatalysis, however, saturation resulted in certain restrictions when solely using AC. The results displayed that the combination of AC removal of toluene and the photocatalytic removal could significantly extend toluene removal duration. In comparing the effectiveness of the two catalyst types it was found that the GB/TiO_2 was half as effective as AC/TiO_2 catalyst for toluene removal.

Voronstov *et al.* [74] also investigated the use of vibration to improve fluidisation of granular photocatalysts for the decomposition of gaseous acetone. A variety of fixed bed constructions were investigated together with the vibrofluidised bed system to enable an efficient comparison. The vibrofluidised bed system was the most effective with an 8.7 % in quantum efficiency being achieved. The high efficiency of the vibrofluidised bed was, interestingly, attributed to the external vibrations used together with the 'periodic light phenomenon'. This phenomenon resulted from the eccentric movement photocatalyst movement within the reactor which consequently enabled increased absorption of scattered light.

A fluidised bed system utilising an upward stream of air which brought TiO_2 pellets to a fluidised state has also been reported [76]. The reactor consisted of a reaction chamber which contained a foraminated member supporting a bed of mobile photocatalysts along with an aeration device to allow for agitation of photocatalytic particles. The aeration device generated gas bubbles through a perforated shelf allowing agitating of photocatalysts. The reactor configuration was utilised for the treatment of waste water in a flow through style process. The reactor concept was designed to reduce or completely remove the need for moving parts, thus allowing for a reactor concept with a reduced foot print suggesting a more energy efficient design. To ensure the constant agitation of the particles the terminal settling velocity of the particles must not exceed the velocity of any upward flow of the liquid through the perforated shelf by more than 10 ms. The reactor retained the advantage of the use of pellets which both allow for reduced downstream processing and via agitation present a number of faces capable of excitation by illumination.

Immobilised Liquid Reactors

Fixed bed

Al-Ekabi and Serpone [77] investigated TiO_2 supported on a glass matrix for the photo-decomposition of phenol, 4-chloropheol, 2,4-dichlorophenol, and 2,4,5-trichlorophenol. The degradation followed first order kinetics with the reaction occurring on the surface of the semiconductor. The irradiation source was an AM-1 filter simulating solar irradiation. A fixed bed reactor system employing a fibre-optic cable (OFR) was reported by Pill and Hoffmann [34]. The system was conceived to allow for remote light distribution to photocatalysts, to effectively determine of quantum yields through effective light flux measurement. Furthermore OFR allowed for reactor reuse to assess different coatings and light input angles, and to minimise potential heating and photocatalyst delamination. They anchored TiO_2 particles onto quartz fibres and light was transmitted to the TiO_2 particles via radial refraction of light out of the fibre. A maximum quantum efficiency of ø = 0.011 for the oxidation of 4-chlorophenol was achieved. This can be compared to a maximum quantum efficiency of ø = 0.0065 for 4-chlorophenol oxidation in a TiO_2 slurry reactor.

This study was followed with an investigation into the application of the OFR system towards the photocatalytic degradation of pentachlorophenol, oxalate and dichloroacetate [34]. Relatively high apparent quantum efficiencies of ø = 0.010, 0.17, and 0.08 were achieved for PCP, OX and DCA respectively, with complete mineralisation reported. It was concluded that the OFR system had the advantages of a fixed-bed unit together with the kinetic efficiency of a slurry reactor. The OFR configuration enhanced the not only the distribution but also the uniformity of activated photocatalyst within a particular reaction volume

compared to standard fixed-bed designs. These characteristics reduced mass transport limitations for photochemical conversion efficiency and allowed higher processing capacities. Furthermore, potential light loss via absorption or scattering by the reaction medium was minimised. The OFR system could be used in batch or continuous flow operation for both liquid and or gas phase reactions. The transmission cable also allowed for remote light delivery to the photocatalyst.

Nogueira and Jardim [78] reported the photodegradation of methylene blue using solar irradiation on a fixed bed reactor with TiO_2 immobilised on a flat glass plate as a support. They investigated the slope of the plate and found that it influenced the methylene blue photodegradation because of 2 factors:

i. the fluid thickness film which flowed over the plate and
ii. the light intensity that reached the system.

They reported a limited range of slopes 22° – 25° and found that 95.8 % of the model compound was degraded at 22° slope while 89 % was degraded at 25° angle. Ray and Beenackers[78] proposed a distributive type fixed bed reactor system that employed hollow glass tubes as of light conductors for distribution to photocatalyst particles. The reactor configuration increased the surface to volume ratio while eliminating the potential light loss through absorption and scattering by reaction matrix. This configuration facilitated a large surface of photocatalyst to be deployed within a relatively small reactor volume. Between 70 and 100 fold increase in surface area per m^3 of reactor volume was achieved compared to a conventional annular reactor configuration. The photo-

degradation of special brilliant blue, a model dye pollutant, was investigated and a 90% photocatalytic destruction of the dye achieved after 100 min irradiation. This study was followed up with the development of a tube light reactor which had a 100-150 fold increase in surface area per unit volume of fluid being treated compared to a conventional annular reactor design and a 10-20 fold increase contrasted with an immersion reactor. In a study of a reactor volume of 3.65×10^{-4} m^3 containing 21 U-shaped lamps of diameter 0.45 cm coated with the a P25 photocatalyst, a 695% increase reactor efficiency was achieved compared with an annular photocatalytic reactor. Furthermore a 259 % increase in efficiency was obtained for the new unite compared with a slurry reactor.

Feitz *et al.* [79] investigated two fixed bed photocatalytic reactors, a packed bed reactor and a coated mesh reactor, using solar illumination. They assessed the processing rate for 2 mg l^{-1} phenol solutions, and calculated a rate of 140 mg m^{-2} h^{-1} for the packed bed reactor with a rate of 20 mg m^{-2} $h^{-1}$for the coated mesh reactor. The lower activity obtained with the coated mesh reactor was believed to be due to insufficient photocatalyst surface contact, low levels of available attached TiO_2 and a small reactor to tank volume ratio. Photonic efficiencies for the decomposition of 100 mg^{-1} dichloroacetic acid solutions using the packed bed unit were only 40% lower than suspension systems. They therefore proposed that this system was particularly effective for treating contaminated water.

Dionysiou *et al.* [80] developed a TiO_2 rotating disk reactor for the decomposition of organic pollutants in water (figure 8). They used a commercial TiO_2 composite ceramic ball photocatalyst material. LiCl tracer studies performed under different disk angular velocities, between 5 and 20 rpm, demonstrated that mixing in the

rotating disk photocatalytic reactor RDPR was similar to that of a continuous stirred tank reactor. They reported the destruction of >90 % 4-Chlorobenzoic acid after 6 hours irradiation. The light intensity distribution within the reactor was also determined and found to vary from about 30 to 1500 μW/cm^2 within the reactor. The RDPR has a number of advantages it eliminates the need for effluent filtration as the catalyst is immobilised, the 3-D nature of the flow created enabled effective mixing, whilst the formation of the thin film allowed more effective oxygen transport from the gas phase to the photocatalyst surface. The photonic efficiency calculated for the experiment at 4 rpm was 2.7 %. The authors anticipate this value to improve with process optimisation[81,82]. A similar study by Hamill *et al*.[82] reported the use of a sealed rotating photocatalytic reactor (RPC) of similar configuration to the Dionysiou RDPR [80, 81, 83]. They investigated the photo-degradation of dichlorobutene and examined the effects of mass transfer and combinations of pollutants. They reported that the RPC could effectively degrade a range of substrates and that the degradation rate was dependent on rotation speed. They also reported that this configuration could be applied to both volatile and non-volatile pollutants.

FIGURE 8

Mehrvar *et al.* [27] reported the use of a photoreactor with TiO_2 coated tellerette packing. The tellerette packings were constructed from stainless steel welding wire which was 'roughened' to promote the adhesion of TiO_2 to the surface. The wires were then wound in a spiral or 'spring like' structure to be formed. The wound wire was cut into smaller lengths and each individual 'spring' adjusted to allow the ends to be brought together to form the tellerete shape. The tellerette type packings were selected and manufactured on the basis that they would

permit sufficient light dispersion into the interior of the bed to maintain effective photocatalytic reaction rates with no significant mass transfer limitations. The photoreactor allowed substantial UV light penetration throughout its interior, and had no significant mass transfer limitations during the photocatalytic degradation of 1,2-dioxane. It was concluded that the range of attenuation coefficients of interest, the reaction rate at various radial positions will not be significantly mass transfer limited unless the photocatalyst activity is increased by at least one order of magnitude.

A novel photocatalytic reaction system, composed of solution and gas spaces that were divided by a thin Teflon film and TiO_2 coated mesh or cloth has been reported[84]. The activity of TiO_2 immobilised on a stainless steel mesh and on a fibre-glass cloth using isopropanol as a model compound was investigated. Although both support materials yielded comparable photocatalytic activities the fibre glass cloth was the most stable. The Teflon membrane enhanced the O_2 levels in the reaction solution which increased the photocatalytic activity for the destruction of organic compounds in water. The benefit of this system for the photo-degradation of aqueous volatile organic carbons was that it did not require air bubbling, which resulted in volatilization of the contaminants to the atmosophere.

Lim *et al.* [68] reported the use of an external lamp, annular photocatalytic reactor with TiO_2 adsorbed on a quartz tube for the degradation of phenanthrene and pyrene from a dilute water stream. They reported that above a feed velocity of 7

cm min^{-1} the process was rate controlled and not influenced by mass transfer limitations.

A tubular photocatalytic reactor for water purification using a ceramic cylindrical tube with a Pt-loaded TiO_2 film coated on the inner surface of the tube has been developed by Zhang *et al* [85]. Phenol, trichloroethylene and bisphenol A were used as model pollutants to examine the effectiveness of the photoreactor. The complete degradation of each pollutant within 2 hours reaction time was observed with the authors concluding that the performance of the reactor was dependent on the aeration of the system.

McMurray *et al*. [86] reported the use of a stirred tank reactor with immobilised Degussa P25 TiO_2 for the degradation of oxalic acid and formic acid. The rate of degradation of both acids was not mass transfer limited with propeller speeds greater than 1000 rpm. They reported apparent quantum yields of 5 % for oxalic acid and 10 % for formic acid.

A sol-gel prepared TiO_2 coating on a tubular photocatalytic reactor with re-circulation mode and a batch photocatalytic reactor was investigated by Lin at al [87] for the degradation of methylene blue and phenol. The sol-gel film synthesised demonstrated an effective photocatalytic activity for the decomposition of organic compounds in water and the authors proposed the use of this reactor for water purification. During a 180 minute photoreaction of phenanthrene, 67.6 % destruction was observed with a 40.1 % conversion to CO_2.

Zhang *et al*.[38] reported the use of a corrugated plate reactor configuration which was developed and assessed using 4-chlorophenol as model pollutant. They compared the new configuration with a flat plate reactor and a slurry reactor. The corrugated plate reactor was reported to be 150 % faster with mass transfer rates 600 % higher than that of a flat plate reactor. The authors suggested that the enhanced performance of the corrugated configuration was a result of the relatively larger illuminated photocatalyst surface area per unit volume, coupled with an effective delivery of both photons and reactants to the photocatalyst surface.

The photocatalytic oxidation of a non ionic surfactant was carried out in a labyrinth flow reactor with an immobilised photocatalyst bed[88]. The work focused on the effects of flow-rate for the decomposition of the non-ionic surfactant. The authors concluded that the optimum photodegradation of the surfactant was observed with a flow-rate of 11.98 dm^3/h. They further studied the remediation of Acid Red 18, an azo dye [89]. Long reaction times were investigated for the photo-degradation of Acid Red using an immobilised Aeroxide Degussa P25 catalyst. Slower flow rates affected the efficiency of the system, with mineralisation times varying from 35 hours to 60 hours depending on flow rate.

An annular photocatalytic reactor, assimilated to a plug flow reactor, with a fixed bed of Degussa P25 immobilised onto a fibre glass support was reported for the remediation of gaseous acetone [26] (figure 9). There was no limitation on mass

transfer observed either internally or externally under the experimental conditions investigated.

FIGURE 9

An internally illuminated monolith reactor (IIMR) has been reported in the investigation of multi-phase photocatalysis [90, 91]. The IIMR had side light emitting fibres incorporated within the channels of a ceramic monolith containing a TiO_2 photocatalyst coated individual channel walls. Photonic efficiencies obtained with this reactor were below those obtained for a slurry reactor but greater than that reported for an annular photoreactor and a reactor configuration with side light fibres immersed in a TiO_2 slurry. The authors reported that the IIMR had a larger area of catalyst exposed to illumination and this is its key advantage over other photocatalytic reactors.

Immobilised Gas Reactors

The use of the Optical Fibre Reactor (OFR) for the photoreduction of CO_2 to fuels by a visible light activated catalyst has been reported by Nguyen and Wu[92]. The optical fibres were coated with a gel-derived TiO_2-SiO_2 mixed photocatalyst. The OFR reactor operated on the principle of incident light being split in two beams when first in contact with the surface of the fibre. Part of the light penetrated the layer of catalyst on the fibre and creates excitation, while the other beam shall reflected off the fibre and transmit along the length of the optical fibre. This allowed the light to gradually spread through the length of the reactor. Two photocatalysts were utilised in this investigation; Cu-Fe/TiO_2 along with Cu-Fe/TiO_2-SiO_2. The products obtained in this study included ethylene and

methane, along with traces of ethane and methanol. The product formation under UVA illumination demonstrated selectivity towards the photocatalyst used, with the exception of methane which was evolved with each of the photocatalysts. The highest rate of methane production, 1.860 µmol/g-cat h was found when the catalyst Cu(0.5 wt.%)-Fe(0.5 wt.%)/TiO_2-SiO_2-acetyl acetone (acac) on optical fibres was used. Ethylene evolution was selective in production and was only seen over Fe and Cu containing catalysts; the highest production rate of 0.575 µmol/g-cat h was found when the catalyst Cu(0.5 wt.%)-Fe(0.5 wt.%)/TiO_2 on optical fibres was used. In comparison natural sunlight (from a solar concentrator) produced a production rate of 0.279 µmol/g-cat h with the catalyst Cu(0.5 wt.%)-Fe(0.5 wt.%)/TiO_2-SiO_2-acac on optical fibres, significantly higher than the rate for the TiO_2-SiO_2 catalyst. These results achieved were attributed to the increased surface area from the use of TiO_2-SiO_2 in comparison to pure TiO_2 and the presence of Cu and Fe metals to shifted the light absorption into the visible spectrum. The benefits of this system included uniform light distribution throughout the reactor, a feature not seen in traditional packed bed designs and the visible light driven catalyst which the authors concluded enhanced the applicability as a commercial and industrial application.

FIGURE 10

Immobilised Vapour Reactors

The development of a cost effective and ease-of-use catalyst support for an immobilised system was investigated by Haijiesmaili *et al*[93]. This investigation focused on TiO_2 being supported upon a 3-dimensional carbon foam for the oxidation of gaseous methanol in a vapour phase flow-through photoreactor. An

impregnation technique was adopted for the production of the TiO_2 supported carbon foam; carbon foam was immersed into a TiO_2 (P25)-containing water/ethanol (1:1) solution followed by drying. The photoreactor was established by packing the carbon foam supported TiO_2 into a Pyrex tube with internal illumination from an 8 W central UV-A light. Results were based upon methanol conversion and CO_2 and formaldehyde selectivity. The methanol conversion with the carbon foam supported TiO_2 was dependent on TiO_2 loading where TiO_2 loadings of 7.7, 9.4, 16.3 and 28.5 wt% achieved methanol conversions of 52, 57, 61 and 75 % respectively. A maximum methanol conversion of 81% was achieved for a 666 wt% TiO_2 loading. These results were impressive compared to those obtained in the photoreactor where the TiO_2 photocatalyst was simply coated on the inside of the reactor wall. In this case the highest methanol conversion reached was 22 %, where after any increase in TiO_2 loading resulted in a screening effect of excess particles and resulted in no further increase in methanol conversion. CO_2 and formaldehyde selectivity further supported the findings in the paper with CO_2 reaching 44 % compared to 7 % wall coated reactor. The efficiency of the carbon foam supported TiO_2 photoreactor was attributed to the ability to increase the exposed surface of the carbon foam and hence increase the surface to reactor ratio which allowed for increasing the TiO_2 content within the reactor. The authors concluded the reactors air to surface ratio and ability to perform at very low pressure drops allow its use in practical applications.

Suspension vs. Immobilised Reactors: A Comparison

Dutta and Ray[28] developed a Taylor vortex photocatalytic reactor that created unsteady Taylor-Couette flow between two co-axial cylinders through re-circulation of fluids from the body of the reator to the inner cylinder wall, coated with TiO_2, (figure 11 a and b). The Taylor-Couette flow is the movement of viscous fluids in between a pair of coaxial cylinders which experience inner centrifugal instability when the inner cylinder rotates differentially with respect to the outer cylinder. They investigated the effect of the Reynolds number (figure 11 c) and catalyst loading on the photodegradation and compared the results with that of a slurry reactor. They noted that increasing the Reynolds number increased the rate of photodegradation of their model pollutant orange II demonstrating that external mass transfer controlled the overall reaction rate, figure 12.

FIGURE 11

The performance of a suspended catalyst system, an immobilised catalyst where the wall of the reactor was coated and an immobilised system packed with coated glass beads has been compared for the photodegradation of formic acid [94]. Mass transfer limitations were observed in the immobilised system with the catalyst coated on the reactor wall. However aerating the system overcame this mass transfer problem. The performance of the packed bed reactor was investigated for two different sized beads (d= 1.3 and 2 mm) to gain an understanding of the photocatalytic activity. The authors concluded that large beads enhanced the photocatalytic activity.

A pilot reactor utilising a TiO_2 coated 15 pores-per-inch alumina reticulated foam monolith incorporated in the space between a centrally deployed UV lamp and

the internal wall of the reactor has been compared with a Degussa P25 TiO_2 slurry system [95]. Results for the degradation of 1,8-diazobicyclo[5.4.0]undec-7-ene (DBU) indicated that the foam monolith immobilised photocatalyst system was more efficient compared to the slurry photocatalyst reactor suggesting that the immobilised system could be scaled up for water purification.

Three different reactor configurations, slurry reactor, wall reactor and fixed-bed reactor, were compared for the photocatalytic disinfection of *Escherichia coli* aqueous suspensions and methylene blue photodegradation (figure 12). Titania was in suspension for the slurry reactor, was immobilised on the reactor wall for the wall reactor and was immobilised on the packing in the fixed bed reactor[96]. The authors investigated the effect of increasing catalyst layer thickness and compared it to increasing concentration of catalyst in the slurry system. The results for methylene blue photo-oxidation were in good agreement for both slurry and immobilised system. For the photocatalytic disinfection, however, this was not the case. The increased density of TiO_2 film caused by the heat treatment reduced the surface area of catalyst available for the micro-organisms and therefore reduced the photocatalytic activity was observed. When the immobilised reactor was investigated for effluents sampled from a wastewater treatment plant, however, they required comparable irradiation times to the slurry system to reach the bacterial detection limit.

FIGURE 12

Industrial Applications

The potential industrial applications for semiconductor photocatalysis are wide and diverse ranging from treating oil and gas effluent to potable water. The reality of research based photoreactor designs are, however, that very few laboratory scale test reactors are ultimately feasible in terms of industrial scale up. In an industrial environment the volume and rate of waste effluent production is in the order of hundreds of cubic meters i.e. millions of litres per day. Typically laboratory photoreactors have a capacity of between 1 ml and 1 L, with a UV illumination source between 36 W and 500 W. Transforming a even 1 L capacity reactor to a 1 m^3 capacity unit is not a simple transformation, with the relationship between materials, volume, catalyst loading, turbidity and UV penetration presenting complex challenges.

Examples where industrial scale photoreactors have been employed on a large scale are those of a solar activated designs. Solar photoreactors have the advantage of not requiring artificial light sources but do require huge amounts of space and are also depend on the solar insolence[97-99].

Pilot Scale Studies

Imoberdorf *et al* [100] propose a scaled up multi-annular photocatalytic reactor for the remediation of air pollution. This consists of four concentric cylindrical borosilicate glass tubes (figure 13). The illumination source, Philips TL18W UV lamp, was placed on the central axis of the system. With the available reaction length of 177 cm the total surface area available for radical production was 5209 cm^2, a significant increase compared to the 81 cm^2 of the laboratory test reactor. Using a sol gel process a thin layer of TiO_2 was coated on two walls of the

reactor which were in contact with the gas flowing through each annulus of the unit.

FIGURE 13

In this study Imoberdorf *et al.* [100] examined the mechanisms of radiative transfer, rate kinetics and mass transfer. They proposed that the process should be free from mass transfer limitations with a reactor operated under the kinetic control. It was found that it was possible to make accurate predictions of reactor behaviour, based purely on the chemical reaction fundamentals, reactor engineering and radiation transport theory. This took no account of the adjustable or unknown parameters of photoreactor design.

Shu and Chang [101] have reported the investigation of a pilot scale thin gap annular plug flow (TGAPF) and photoreactor and recirculated batch reactor for the degradation of azo dye waste water using H_2O_2 instead of a semiconductor photocatalyst. The TGAPF system was tested using acid orange 10 at a concentration of 20 mg/L^{-1} with a simulated waste water prepared in a tank reservoir at a volume of 100 L. The TGAPF reactor having a capacity of 3000 ml and the dye was pumped through the TGAPF reactor at a rate of 1.5 L/min^{-1} to 6.5 L/min^{-1}, which gave a through put of 2.35 – 9.32 m^3 day^{-1}. The UV lamp source was a 5000 W medium pressure mercury at 253.7 nm and was positioned centrally in the quartz housing. This configuration allowed a azo dye degradation rate of 0.26 min per L of dye to 99% of original concentration, e.g. 100 L in 26.9 min. When compared to the degradation rate of the recirculated batch reactor the TGAPF reactor was 233 times more efficient, with the batch reactor taking 6267 min to degrade the same volume and concentration of azo dye.

These two examples of scaled up pilot photoreactors show that there is the potential for increasing capacity, although it is worth noting that the Shu and Chang TGAPF reactor does require a 5000 W UV source which is both expensive and has significant associated operating costs.

The double skin sheet reactor (DSSR) comprises a flat transparent box framework constructed from PLEXIGLAS® [98, 102](figure 14). The photocatalyst was deployed as a suspension in the waste water and the slurry was then pumped through the channels of the unit. After the degradation process the photocatalyst had to be removed from the suspension either by filtering or by sedimentation. The DSSR has been demonstrated to utilize both direct and the diffuse portion of solar radiation. A pilot scale DSSR, has been investigated for the treatment of industrial wastewater effluent in Wolfsburg, Germany[99]. 50 % of the organic pollutants in the waste water were degraded within between eight and eleven hours irradiation. The efficiency of the photocatalytic process was found to be dependent on the initial pollutant concentration, the time of illumination, and, not surprisingly, the solar UV light flux density.

FIGURE 14

Conclusions

The research detailed in this review highlight the diversity in photocatalytic reactor design along with their potential applications. Suspended Liquid Reactors, Immobilised Liquid Reactors, Immobilised Gas Reactors and

Immobilised Vapour were considered and, where appropriate, compared in an attempt to address the advantages and disadvantages of individual designs.

The following conclusions could be drawn from considering the current state of the art in this field;

1. Slurry and suspended systems offer the advantage of increased surface area allowing increased photocatalyst and reactant interaction and has proved effective in the treatment of wastewater. Limited light penetration and downstream processing procedures, particularly with respect to catalyst separation, however, restrict these concepts for commercialisation and scale up.

2. Fluidised bed reactors also present excellent photocatalyst surface area to pollutant ratios for photocatalytic transformations. Research has demonstrated that these systems have been effective for both gas and liquid phase photocatalysis. This has enabled the use of highly efficient powders such as Degussa P25 which benefit from the ‘periodic light phenomenon’ created by fluidised systems. Drawbacks to the system include the loss or ‘drifting’ of particles within the system and downstream processing restrictions.

3. Fixed bed designs utilise immobilised catalysts which have the advantages of no downstream processing restrictions such as separation and filtration and allow operation on both a batch and continuous flow phase. There are restrictions regarding this system including difficulty in the illumination of the entire support containing the catalyst and mass transfer limitations

affected by catalyst thickness. Furthermore in order to achieve and effective surface area of photocatalyst relative to the effluent being treated, scaled up units require a significant “footprint”.

4. Comparisons of the systems demonstrate that given the correct parameters the individual concepts are effective. While many comparisons of systems describe the immobilised catalyst reactor set-up as having decreased efficiency or restrictions due to mass transfer limitations, it was reported that if such restrictions were overcome results were comparable to that slurry and fluidisation systems.

As has been demonstrated here, a vast array of photoreactor concepts have been reported, all displaying varying engineering characteristics in terms of efficiency for pollutant transport, photocatalyst deployment and activation. These characteristics are all critical however the future of photoreactor technology does not solely rely in the design of the reactor itself, but in the development of more effective photocatalysts, particularly in rate limited systems. The development of photocatalysts that can achieve greater conversion efficiencies at lower irradiation energies, and ultimately visible light absorbing materials will be a critical component in ensuring wide scale adoption of this versatile technology. For industrial applications photoreactors need to meet the challenge of capacity, ruggedness, reliability and ease of use. Currently the only design of photoreactor which is capable of processing the level of waste water required is that of suspension reactors, but as noted in this review they are far from infallible. Ultimately however, the application of

semiconductor photocatalysis for remediation is has real scope for impacting on water pollution and hence global water scarcity.

References.

1. Ollis DF, Al-Ekhabi, H., Photocatalytic purification and treatment of water and air. *Elsevier* (1993).
2. Mills A and Le Hunte S, An overview of semiconductor photocatalysis. *Journal of Photochemistry and Photobiology A: Chemistry* **108**: 1-35 (1997).
3. Hoffman AJ, Carraway ER and Hoffmann MR, Photocatalytic Production of H2O2 and Organic Peroxides on Quantum-Sized Semiconductor Colloids. *Environmental Science & Technology* **28**: 776-785 (1994).
4. Fox MA and Dulay MT, Heterogeneous photocatalysis. *Chemical Reviews* **93**: 341-357 (1993).
5. Fujishima A, Rao TN and Tryk DA, Titanium dioxide photocatalysis. *Journal of Photochemistry and Photobiology C: Photochemistry Reviews* **1**: 1-21 (2000).
6. Ireland JC, Klostermann P, Rice EW and R M Clark RM, Inactivation of Escherichia coli by titanium dioxide photocatalytic oxidation. *Applied Environmental Microbiology* **59**: 1668-1670 (1993).
7. McCullagh C, Robertson J, Bahnemann D and Robertson P, The application of TiO_2 photocatalysis for disinfection of water contaminated with pathogenic micro-organisms: a review. *Research on Chemical Intermediates* **33**: 359-375 (2007).
8. Sjogren JC, and Sierka, R.A., Inactivation of phage ms2 by iron-aided titanium dioxide photocatalysis. *Applied and Envrionmental Microbiology* **60**: 344-347 (1994).
9. Cai R, Hashimoto, K. Kubota, Y. and Fujishima, A. , Increment of Photocatalytic Killing of Cancer Cells Using TiO2 with the Aid of Superoxide Dismutase. *Chemistry Lett* (1992).
10. Cai R, Kuboata, Y., Shuin, T., Hashimoto, K., and Fujishima, A., Induction of Cytotoxicity by Photo-excited TiO2 Particles. *Cancer Res*: 2346-2348 (1992).
11. Fujishima A and Honda K, Electrochemical Photolysis of Water at a Semiconductor Electrode. *Nature* **238**: 37-38 (1972).
12. Karakitsou KE and Verykios XE, Effects of altervalent cation doping of titania on its performance as a photocatalyst for water cleavage. *J Phys Chem* **97**: 1184-1189. (1993).
13. Suzuki in, Photocatalytic purification and treatment of water and air. *Eds Ollis, David F, Al-Ekhabi, H Elsevier* (1993).
14. Borgarello E, Kiwi J, Pelizzetti E, Visca M and Gratzel M, Photochemical cleavage of water by photocatalysis. *Nature* **289**: 158-160 (1981).
15. Taqui Khan MM and Nageswara Rao N, Stepwise reduction of coordinated dinitrogen to ammonia via diazinido and hydrazido intermediates on a visible light irradiated Pt/CdS · Ag2S/RuO2 particulate system suspended in an aqueous solution of K[Ru(EDTA-H)Cl]2H2O. *Journal of Photochemistry and Photobiology A: Chemistry* **56**: 101-111 (1991).
16. Schiavello M, Some working principles of heterogeneous photocatalysis by semiconductors. *Electrochimica Acta* **38**: 11-14 (1993).
17. Taqui Khan MM, Chatterjee D and Bala M, Photocatalytic reduction of N2 to NH 3 sensitized by the [RuIII-ethylenediaminetetraacetate-2,2'-

bipyridyl]- complex in a Pt-TiO2 semiconductor particulate system. *Journal of Photochemistry and Photobiology A: Chemistry* **67**: 349-352 (1992).
18. Khan MMT, Chatterjee D, Krishnaratnam M and Bala M, Photosensitized reduction of N_2 by RuII(bipy)$_3^{2+}$ adsorbed on the surface of Pt/TiO_2/RuO_2 semiconductor particulate system containing RuIII-EDTA complex and L-ascorbic acid. *Journal of Molecular Catalysis* **72**: 13-18 (1992).
19. Gerischer H, Heller, A. , Photocatalytic oxidation of organic molecules at titanium dioxide particles by sunlight in aerated water. *J Electrochem Soc* **139** (1992).
20. Jackson NB, Wang, C. M., Luo, Z., Schwitzgebel, J., Ekerdt, J. G., Brock, J. R., Heller, A., Attachment of TiO2 Powders to Hollow Glass Microbeads: Activity of the TiO2-Coated Beads in the Photoassisted Oxidation of Ethanol to Acetaldehyde. *J Electrochem Soc* **138**: 3660-3664 (1992).
21. Nair M, Luo Z and Heller A, Rates of photocatalytic oxidation of crude oil on salt water on buoyant, cenosphere-attached titanium dioxide. *Industrial & Engineering Chemistry Research* **32**: 2318-2323 (1993).
22. Boer KW, Survey of semiconductor physics. *Van Nostrand, New York*: 1472 (1990).
23. Kormann C, Bahnemann DW and Hoffmann MR, Photocatalytic production of hydrogen peroxides and organic peroxides in aqueous suspensions of titanium dioxide, zinc oxide, and desert sand. *Environmental Science & Technology* **22**: 798-806 (1988).
24. Carraway ER, Hoffman AJ and Hoffmann MR, Photocatalytic Oxidation of Organic Acids on Quantum-Sized Semiconductor Colloids. *Environmental Science & Technology* **28**: 786-793 (1994).
25. Mohseni M, Gas phase trichloroethylene (TCE) photooxidation and byproduct formation: photolysis vs. titania/silica based photocatalysis. *Chemosphere* **59**: 335-342 (2005).
26. Vincent G, Marquaire PM and Zahraa O, Abatement of volatile organic compounds using an annular photocatalytic reactor: Study of gaseous acetone. *Journal of Photochemistry and Photobiology A: Chemistry* **197**: 177-189 (2008).
27. Mehrvar M, Anderson WA and Moo-Young M, Preliminary analysis of a tellerette packed-bed photocatalytic reactor. *Advances in Environmental Research* **6**: 411-418 (2002).
28. Dutta PK and Ray AK, Experimental investigation of Taylor vortex photocatalytic reactor for water purification. *Chemical Engineering Science* **59**: 5249-5259 (2004).
29. Sczechowski JG, Koval CA and Noble RD, A Taylor vortex reactor for heterogeneous photocatalysis. *Chemical Engineering Science* **50**: 3163-3173 (1995).
30. Giordano RC, Giordano RLC, Prazeres DMF and Cooney CL, Analysis of a Taylor-Poiseuille vortex flow reactor--I: Flow patterns and mass transfer characteristics. *Chemical Engineering Science* **53**: 3635-3652 (1998).
31. Richter O, Hoffmann H and Kraushaar-Czarnetzki B, Effect of the rotor shape on the mixing characteristics of a continuous flow Taylor-vortex reactor. *Chemical Engineering Science* **63**: 3504-3513 (2008).
32. Kuo HP, Wu CT and Hsu RC, Continuous reduction of toluene vapours from the contaminated gas stream in a fluidised bed photoreactor. *Powder Technology* **195**: 50-56 (2009).

33. Lee D-K, Kim S-C, Cho I-C, Kim S-J and Kim S-W, Photocatalytic oxidation of microcystin-LR in a fluidized bed reactor having TiO2-coated activated carbon. *Separation and Purification Technology* **34**: 59-66 (2004).
34. Peill NJ and Hoffmann MR, Development and Optimization of a TiO2-Coated Fiber-Optic Cable Reactor: Photocatalytic Degradation of 4-Chlorophenol. *Environmental Science & Technology* **29**: 2974-2981 (1995).
35. Li Puma G and Yue PL, Comparison of the Effectiveness of Photon-Based Oxidation Processes in a Pilot Falling Film Photoreactor. *Environmental Science & Technology* **33**: 3210-3216 (1999).
36. D. Bockelmann RG, D. Weichgrebe, and D. Bahnemann, Solar detoxification of polluted water: comparing the efficiencies of a parabolic through reactor and a novel thin-film fixed-bed reactor. *In Photocatalytic Purification and Treatment of Water and Air, D F Ollis and H Al-Ekabi, Eds, Elsevier Science, Amsterdam, The Netherlands* pp. 771-776 (1993).
37. Sahle-Demessie E, Bekele S and Pillai UR, Residence time distribution of fluids in stirred annular photoreactor. *Catalysis Today* **88**: 61-72 (2003).
38. Zhang Z, Anderson WA and Moo-Young M, Experimental analysis of a corrugated plate photocatalytic reactor. *Chemical Engineering Journal* **99**: 145-152 (2004).
39. Dijkstra MFJ, Michorius A, Buwalda H, Panneman HJ, Winkelman JGM and Beenackers AACM, Comparison of the efficiency of immobilized and suspended systems in photocatalytic degradation. *Catalysis Today* **66**: 487-494 (2001).
40. Chong MN, Jin B, Zhu HY, Chow CWK and Saint C, Application of H-titanate nanofibers for degradation of Congo Red in an annular slurry photoreactor. *Chemical Engineering Journal* **150**: 49-54 (2009).
41. Augugliaro V, Loddo V, Palmisano L and Schiavello M, Performance of Heterogeneous Photocatalytic Systems: Influence of Operational Variables on Photoactivity of Aqueous Suspension of TiO2. *Journal of Catalysis* **153**: 32-40 (1995).
42. Minero C and Vione D, A quantitative evalution of the photocatalytic performance of TiO2 slurries. *Applied Catalysis B: Environmental* **67**: 257-269 (2006).
43. Ollis DF, Pelizzetti, E., Serpone, N., Photocatalyzed destruction of water contaminants. *Environmental Science & Technology* **25**: 1522-1529 (1991).
44. Ray AK and Beenackers AACM, Novel swirl-flow reactor for kinetic studies of semiconductor photocatalysis. *AIChE Journal* **43**: 2571-2578 (1997).
45. Chen D, Li F and Ray AK, External and internal mass transfer effect on photocatalytic degradation. *Catalysis Today* **66**: 475-485 (2001).
46. Pruden AL and Ollis DF, Degradation of chloroform by photoassisted heterogeneous catalysis in dilute aqueous suspensions of titanium dioxide. *Environmental Science & Technology* **17**: 628-631 (1983).
47. Kormann C, Bahnemann DW and Hoffmann MR, Photolysis of chloroform and other organic molecules in aqueous titanium dioxide suspensions. *Environmental Science & Technology* **25**: 494-500 (1991).
48. Pramauro E, Vincenti M, Augugliaro V and Palmisano L, Photocatalytic degradation of Monuron in aqueous titanium dioxide dispersions. *Environmental Science & Technology* **27**: 1790-1795 (1993).

49. Pathirana HMKK and Maithreepala RA, Photodegradation of 3,4-dichloropropionamide in aqueous TiO2 suspensions. *Journal of Photochemistry and Photobiology A: Chemistry* **102**: 273-277 (1997).
50. Li Puma G and Yue PL, Photocatalytic Oxidation of Chlorophenols in Single-Component and Multicomponent Systems. *Industrial & Engineering Chemistry Research* **38**: 3238-3245 (1999).
51. Li Puma G and Yue PL, Enhanced Photocatalysis in a Pilot Laminar Falling Film Slurry Reactor. *Industrial & Engineering Chemistry Research* **38**: 3246-3254 (1999).
52. San N, Hatipoglu A, Koçtürk G and ÇInar Z, Prediction of primary intermediates and the photodegradation kinetics of 3-aminophenol in aqueous TiO2 suspensions. *Journal of Photochemistry and Photobiology A: Chemistry* **139**: 225-232 (2001).
53. Jeon J, Kim S, Lim T and Lee D, Degradation of trichloroethylene by photocatalysis in an internally circulating slurry bubble column reactor. *Chemosphere* **60**: 1162-1168 (2005).
54. Sauer T, Cesconeto Neto G, José HJ and Moreira RFPM, Kinetics of photocatalytic degradation of reactive dyes in a TiO2 slurry reactor. *Journal of Photochemistry and Photobiology A: Chemistry* **149**: 147-154 (2002).
55. Kamble SP, Sawant SB and Pangarkar VG, Photocatalytic Mineralization of Phenoxyacetic Acid Using Concentrated Solar Radiation and Titanium Dioxide in Slurry Photoreactor. *Chemical Engineering Research and Design* **84**: 355-362 (2006).
56. Adams M, Campbell, I., Robertson, P.K.J., Novel Photocatalytic Reactor Development for Removal of Hydrocarbons from Water. *International Journal of Photoenergy* **Volume 2008** 7 pages (2008).
57. Author, Apparatus and method for treating a fluid by means of a transparent container (2006).
58. McCullagh C, Robertson PKJ, Adams M, Pollard PM and Mohammed A, Development of a slurry continuous flow reactor for photocatalytic treatment of industrial waste water. *Journal of Photochemistry and Photobiology A: Chemistry* **211**: 42-46 (2010).
59. Salu OA, Adams, M., Robertson, P.K.J., Wong, L.S., and McCullagh, C., Remediation of oily wastewater from an interceptor tank using a novel photocatalytic drum reactor
Desalination and Water Treatment **In Press** (2010).
60. Chen D and Ray AK, Photocatalytic kinetics of phenol and its derivatives over UV irradiated TiO2. *Applied Catalysis B: Environmental* **23**: 143-157 (1999).
61. Martin ST, Herrmann, Hartmut, Choi, Wonyong, Hoffmann, Michael R., Time-resolved microwave conductivity. Part 1.-TiO2 photoreactivity and size quantization. *Journal of the Chemical Society, Faraday Transactions* **90**: 3315-3322 (1994).
62. Mehrotra K, Yablonsky GS and Ray AK, Kinetic Studies of Photocatalytic Degradation in a TiO2 Slurry System:â€‰ Distinguishing Working Regimes and Determining Rate Dependences. *Industrial & Engineering Chemistry Research* **42**: 2273-2281 (2003).
63. Moreira R, Sauer T, Casaril L and Humeres E, Mass transfer and photocatalytic degradation of leather dye using TiO/UV. *Journal of Applied Electrochemistry* **35**: 821-829 (2005).

64. Ballari MdlM, Alfano OM and Cassano AE, Mass transfer limitations in slurry photocatalytic reactors: Experimental validation. *Chemical Engineering Science* **65**: 4931-4942 (2010).
65. Paz Y, Application of TiO2 photocatalysis for air treatment: Patents' overview. *Applied Catalysis B: Environmental* **99**: 448-460 (2010).
66. Dibble LA and Raupp GB, Fluidized-bed photocatalytic oxidation of trichloroethylene in contaminated air streams. *Environmental Science & Technology* **26**: 492-495 (1992).
67. Lim TH and Kim SD, Trichloroethylene degradation by photocatalysis in annular flow and annulus fluidized bed photoreactors. *Chemosphere* **54**: 305-312 (2004).
68. Lim TH and Kim SD, Photocatalytic degradation of trichloroethylene (TCE) over TiO2/silica gel in a circulating fluidized bed (CFB) photoreactor. *Chemical Engineering and Processing* **44**: 327-334 (2005).
69. Coates NH and Rice RL, Sulfur dioxide reduction by combustion of coal in fluidized bed of limestone. *AIChE Symp Ser* **70** (1974).
70. Son Y-H, Jeon, M-K., Ban, J-Y.,Kang, M and Choung, S-J, Application of three-phase fluidized photocatalytic system to decompostions of acetic acid and ammonia. *J Ind Eng Chem* **11**: 938-944 (2005).
71. Kang M, Synthesis of Fe/TiO2 photocatalyst with nanometer size by solvothermal method and the effect of H2O addition on structural stability and photodecomposition of methanol. *Journal of Molecular Catalysis A: Chemical* **197**: 173-183 (2003).
72. Nelson RJ, Flakker CL and Muggli DS, Photocatalytic oxidation of methanol using titania-based fluidized beds. *Applied Catalysis B: Environmental* **69**: 189-195 (2007).
73. Yao G-h, Wang F, Wang X-b and Gui K-t, Magnetic field effects on selective catalytic reduction of NO by NH_3 over Fe_2O_3 catalyst in a magnetically fluidized bed. *Energy* **35**: 2295-2300 (2010).
74. Vorontsov AV, N. Savinov E and Smirniotis PG, Vibrofluidized- and fixed-bed photocatalytic reactors: case of gaseous acetone photooxidation. *Chemical Engineering Science* **55**: 5089-5098 (2000).
75. Lim TH, Jeong SM, Kim SD and Gyenis J, Photocatalytic decomposition of NO by TiO2 particles. *Journal of Photochemistry and Photobiology A: Chemistry* **134**: 209-217 (2000).
76. Foster NR, Bassiti, K., Photocatalytic Reactor. *European Patent - EP2089328 (A1), World Patent - WO2008050119(1998)* (2008).
77. Al-Ekabi H and Serpone N, Kinetics studies in heterogeneous photocatalysis. I. Photocatalytic degradation of chlorinated phenols in aerated aqueous solutions over titania supported on a glass matrix. *The Journal of Physical Chemistry* **92**: 5726-5731 (1988).
78. Nogueira RFP and Jardim WF, TiO2-fixed-bed reactor for water decontamination using solar light. *Solar Energy* **56**: 471-477 (1996).
79. Feitz AJ, Boyden BH and Waite TD, Evaluation of two solar pilot scale fixed-bed photocatalytic reactors. *Water Research* **34**: 3927-3932 (2000).
80. Dionysiou DD, Balasubramanian G, Suidan MT, Khodadoust AP, Baudin I and Laîné J-M, Rotating disk photocatalytic reactor: development, characterization, and evaluation for the destruction of organic pollutants in water. *Water Research* **34**: 2927-2940 (2000).
81. Dionysiou DD, Khodadoust AP, Kern AM, Suidan MT, Baudin I and Laîné J-M, Continuous-mode photocatalytic degradation of chlorinated phenols

and pesticides in water using a bench-scale TiO2 rotating disk reactor. *Applied Catalysis B: Environmental* **24**: 139-155 (2000).
82. Hamill NA, Weatherley LR and Hardacre C, Use of a batch rotating photocatalytic contactor for the degradation of organic pollutants in wastewater. *Applied Catalysis B: Environmental* **30**: 49-60 (2001).
83. Dionysiou DD, Suidan MT, Baudin I and Laîné J-M, Oxidation of organic contaminants in a rotating disk photocatalytic reactor: reaction kinetics in the liquid phase and the role of mass transfer based on the dimensionless Damköhler number. *Applied Catalysis B: Environmental* **38**: 1-16 (2002).
84. Villacres R, Ikeda S, Torimoto T and Ohtani B, Development of a novel photocatalytic reaction system for oxidative decomposition of volatile organic compounds in water with enhanced aeration. *Journal of Photochemistry and Photobiology A: Chemistry* **160**: 121-126 (2003).
85. Zhang L, Kanki T, Sano N and Toyoda A, Development of TiO_2 photocatalyst reaction for water purification. *Separation and Purification Technology* **31**: 105-110 (2003).
86. McMurray TA, Byrne JA, Dunlop PSM, Winkelman JGM, Eggins BR and McAdams ET, Intrinsic kinetics of photocatalytic oxidation of formic and oxalic acid on immobilised TiO2 films. *Applied Catalysis A: General* **262**: 105-110 (2004).
87. Lin HF and Valsaraj KT, A titania thin film annular photocatalytic reactor for the degradation of polycyclic aromatic hydrocarbons in dilute water streams. *Journal of Hazardous Materials* **99**: 203-219 (2003).
88. Mozia S, Tomaszewska M and Morawski AW, Photocatalytic degradation of azo-dye Acid Red 18. *Desalination* **185**: 449-456 (2005).
89. Mozia S, Tomaszewska M and Morawski AW, Photodegradation of azo dye Acid Red 18 in a quartz labyrinth flow reactor with immobilized TiO2 bed. *Dyes and Pigments* **75**: 60-66 (2007).
90. Du P, Carneiro JT, Moulijn JA and Mul G, A novel photocatalytic monolith reactor for multiphase heterogeneous photocatalysis. *Applied Catalysis A: General* **334**: 119-128 (2008).
91. Carneiro JT, Berger R, Moulijn JA and Mul G, An internally illuminated monolith reactor: Pros and cons relative to a slurry reactor. *Catalysis Today* **147**: S324-S329 (2009).
92. Nguyen T-V and Wu JCS, Photoreduction of CO2 to fuels under sunlight using optical-fiber reactor. *Solar Energy Materials and Solar Cells* **92**: 864-872 (2008).
93. Hajiesmaili S, Josset S, Bégin D, Pham-Huu C, Keller N and Keller V, 3D solid carbon foam-based photocatalytic materials for vapor phase flow-through structured photoreactors. *Applied Catalysis A: General* **382**: 122-130.
94. Salaices M, Serrano B and de Lasa HI, Experimental evaluation of photon absorption in an aqueous TiO2 slurry reactor. *Chemical Engineering Journal* **90**: 219-229 (2002).
95. Ochuma IJ, Osibo OO, Fishwick RP, Pollington S, Wagland A, Wood J and Winterbottom JM, Three-phase photocatalysis using suspended titania and titania supported on a reticulated foam monolith for water purification. *Catalysis Today* **128**: 100-107 (2007).
96. van Grieken R, Marugán J, Sordo C and Pablos C, Comparison of the photocatalytic disinfection of E. coli suspensions in slurry, wall and fixed-bed reactors. *Catalysis Today* **144**: 48-54 (2009).

97. Dillert R, Cassano AE, Goslich R and Bahnemann D, Large scale studies in solar catalytic wastewater treatment. *Catalysis Today* **54**: 267-282 (1999).
98. Benz V, Müller, M., Bahnemann, D.W., Weichgrebe, D., Brehm, M., Reaktoren für die photokatalytische Abwasserreinigung mit Stegmehrfachplatten als Solarelemente. *Deutsche Offenlegungsschrift* **DE 195 14 372 A1** (1996).
99. Dillert R, Vollmer, S., Gross, E., Schober, M., Bahnemann, D., Wienefeld, J., Pahlmann, K., Schmedding, T., Arntz, H.-J., Sager, G., Solar-catalytic treatment of an industrial wastewater. *Zeitschrift fur Physikalische Chemie* **213**: 141-147 (1999).
100. Imoberdorf GE, Cassano AE, Irazoqui HA and Alfano OM, Optimal design and modeling of annular photocatalytic wall reactors. *Catalysis Today* **129**: 118-126 (2007).
101. Shu H-Y and Chang M-C, Pilot scale annular plug flow photoreactor by UV/H2O2 for the decolorization of azo dye wastewater. *Journal of Hazardous Materials* **125**: 244-251 (2005).
102. van Well M, Dillert RHG, Bahnemann DW, Benz VW and Mueller MA, A Novel Nonconcentrating Reactor for Solar Water Detoxification. *Journal of Solar Energy Engineering* **119**: 114-119 (1997).
103. Mozia S, Morawski AW, Toyoda M and Inagaki M, Effectiveness of photodecomposition of an azo dye on a novel anatase-phase TiO2 and two commercial photocatalysts in a photocatalytic membrane reactor (PMR). *Separation and Purification Technology* **63**: 386-391 (2008).
104. Alexiadis A and Mazzarino I, Design guidelines for fixed-bed photocatalytic reactors. *Chemical Engineering and Processing* **44**: 453-459 (2005).
105. Cernigoj U, Stangar UL and Trebse P, Evaluation of a novel Carberry type photoreactor for the degradation of organic pollutants in water. *Journal of Photochemistry and Photobiology A: Chemistry* **188**: 169-176 (2007).
106. Lo C-C, Hung C-H, Yuan C-S and Wu J-F, Photoreduction of carbon dioxide with H2 and H2O over TiO2 and ZrO2 in a circulated photocatalytic reactor. *Solar Energy Materials and Solar Cells* **91**: 1765-1774 (2007).
107. Fu J, Ji M, Zhao Y and Wang L, Kinetics of aqueous photocatalytic oxidation of fulvic acids in a photocatalysis-ultrafiltration reactor (PUR). *Separation and Purification Technology* **50**: 107-113 (2006).
108. Li Puma G and Lock Yue P, The modeling of a fountain photocatalytic reactor with a parabolic profile. *Chemical Engineering Science* **56**: 721-726 (2001).
109. Agarwal A and Bhaskarwar AN, Comparative simulation of falling-film and parallel-film reactors for photocatalytic production of hydrogen. *International Journal of Hydrogen Energy* **32**: 2764-2775 (2007).
110. Ochuma IJ, Fishwick RP, Wood J and Winterbottom JM, Photocatalytic oxidation of 2,4,6-trichlorophenol in water using a cocurrent downflow contactor reactor (CDCR). *Journal of Hazardous Materials* **144**: 627-633 (2007).
111. Chin SS, Lim TM, Chiang K and Fane AG, Hybrid low-pressure submerged membrane photoreactor for the removal of bisphenol A. *Desalination* **202**: 253-261 (2007).
112. Orozco SL, Arancibia-Bulnes CA and Suárez-Parra R, Radiation absorption and degradation of an azo dye in a hybrid photocatalytic reactor. *Chemical Engineering Science* **64**: 2173-2185 (2009).

113. Erdei L, Arecrachakul N and Vigneswaran S, A combined photocatalytic slurry reactor-immersed membrane module system for advanced wastewater treatment. *Separation and Purification Technology* **62**: 382-388 (2008).
114. Hao X-g, Li H-h, Zhang Z-l, Fan C-m, Liu S-b and Sun Y-p, Modeling and experimentation of a novel labyrinth bubble photoreactor for degradation of organic pollutant. *Chemical Engineering Research and Design* **87**: 1604-1611 (2009).
115. Pourahmad A, Sohrabnezhad S and Kashefian E, AgBr/nanoAlMCM-41 visible light photocatalyst for degradation of methylene blue dye. *Spectrochimica Acta Part A: Molecular and Biomolecular Spectroscopy* **77**: 1108-1114.
116. Shifu C, Wei Z, Wei L, Huaye Z, Xiaoling Y and Yinghao C, Preparation, characterization and activity evaluation of p-n junction photocatalyst p-CaFe2O4/n-Ag3VO4 under visible light irradiation. *Journal of Hazardous Materials* **172**: 1415-1423 (2009).
117. Liu W, Ji M and Chen S, Preparation, characterization and activity evaluation of Ag2Mo4O13 photocatalyst. *Journal of Hazardous Materials* **186**: 2001-2008.
118. Kanade KG, Baeg J-O, Kale BB, Mi Lee S, Moon S-J and Kong K-j, Rose-red color oxynitride Nb2Zr6O17-xNx: A visible light photocatalyst to hydrogen production. *International Journal of Hydrogen Energy* **32**: 4678-4684 (2007).
119. Jing D, Liu M, Chen Q and Guo L, Efficient photocatalytic hydrogen production under visible light over a novel W-based ternary chalcogenide photocatalyst prepared by a hydrothermal process. *International Journal of Hydrogen Energy* **35**: 8521-8527.
120. Shen S, Zhao L and Guo L, Cetyltrimethylammoniumbromide (CTAB)-assisted hydrothermal synthesis of ZnIn2S4 as an efficient visible-light-driven photocatalyst for hydrogen production. *International Journal of Hydrogen Energy* **33**: 4501-4510 (2008).

Reactor Type	Reactant Phase	Reactor Name	Experimentation	Catalyst Used	Industrial Application/ Comments	Reference
Immobilised	Liquid	Photocatalytic Membrane Reactor (PMR)	Azo dye degredation	Anatase-phase TiO_2		[103]
		Fixed Bed	Waste water treatment	TiO_2		[104]
		Corrugated plate	4-chlorophenol degradation	TiO_2 (P25)		[38]
		Rotating Disc	4-Chlorobenzoic acid degradation	TiO_2 (coated commercial ceramic and glass balls)		[80]
		Carberry photoreactor	4-chlorophenol degradation	TiO_2 (P25) on sodium glass support.		[105]
		Optical Fibre Reactor (OFR)	Degradation of 4-chlorophenol	TiO_2 on quartz fiber cores	Water treatment	[34]
	Gas	Annular Wall	PCE degradation	TiO_2	Air purification	[100]
		Circulated system	CO_2 reduction	TiO_2 (P25), ZrO_2		[106]
		Monolith	Cyclohexane	TiO_2 (Hombikat UV100)	Air purification	[90]
	Vapour	Carbon foam-based photoreactor	Gaseous methanol oxidation	TiO_2 (P25) supported on carbon foam		[93]

Reactor Type	Reactant phase	Reactor Name	Experimentation	Catalyst Used	Industrial Application/ comments	Reference
Suspended	Liquid	Photocatalysis-Ultrafiltration Reactor (PUR)	Fulvic Acid	TiO_2 (P25)		[107]
		Rotating Drum Reactor	Hydrocarbons	TiO_2 (P25)	Waterwater Treatment. Drinking water disinfection.	[56]
		Taylor Vortex	Formate acid	TiO_2 (P25)		[29]
		Fountain	Indigo carmine oxidation	TiO_2		[108]
		Falling film slurry	Salicylic acid oxidation	TiO_2 (P25)		[51]
			Hydrogen production	CdS		[109]
		Internally circulating slurry bubble column reactor	TCE	TiO_2 (P25)		[53]
		Cocurrent downflow contactor reactor (CDCR)	2,4,6-trichlorophenol (2,3,6-TCP)	TiO_2 (VP Aeroperl P25/20)		[110]
		Hybrid low-pressure submerged membrane photoreactor	Removal of bisphenol A	TiO_2 (P25)		[111]
		Hybrid photoreactor	Azo dye – reactive blue 69	TiO_2 (P25)	Wastewater treatment. Uses Solar irradiation	[112]
		Slurry reactor-immersed membrane	Synthetic wastewater	TiO_2 (P25)	Wastewater Treatment	[113]
		Novel labyrinth bubble photocatalytic reactor	Methyl orange degradation	TiO_2 immobilised on quartz glass. (Used in suspension)	Wastewater treatment. Built on a commercial scale.	[114]
		Fluidised bed photoreactor	MC-LR destruction	TiO_2 coated activated carbon		[33]
		Standard slurry photoreactor	Methylene blue degradation	AgBr/nanoAlMCM-41	Visible light activated.	[115]
				p-CaFe2O4/n-Ag3VO4	Visible light activated.	[116]

			Methyl orange oxidation	$Ag_2Mo_4O_{13}$		[117]
			Hydrogen production	$Nb_2Zr_6O_{17-x}N_x$	Visible light activated	[118]
				Cu_2WS_4	Visible light activated	[119]
				$ZnIn_2S_4$	Visible light activated	[120]

Table 1: Overview of photoreactor type, reactant phase, experimental targets, catalyst employed and industrial applications.

Figure 1:

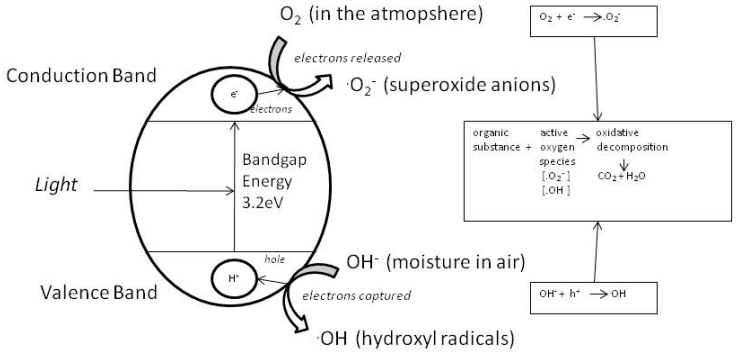

Figure 2:

(A)

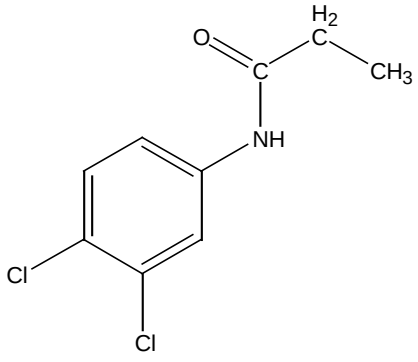

(B)

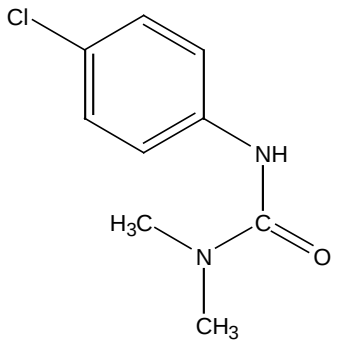

Figure 3:

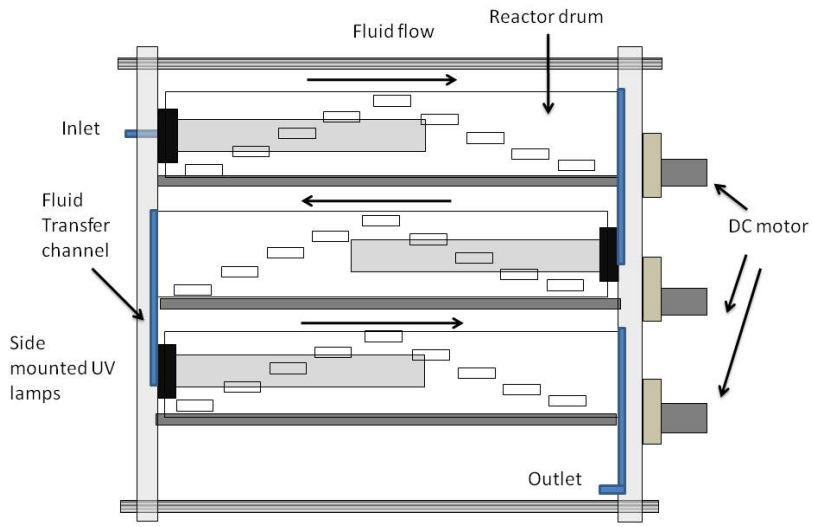

Figure 4:

(A)

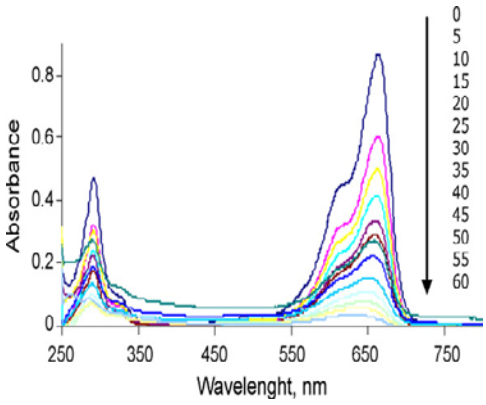

(B)

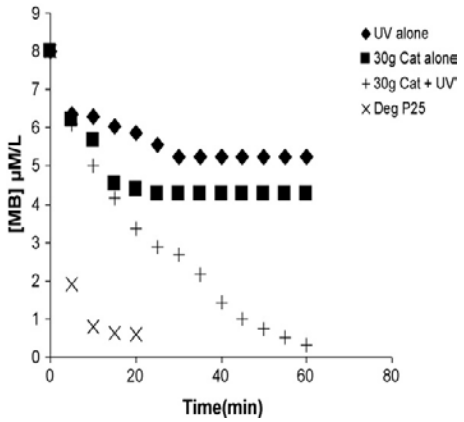

Figure 5:

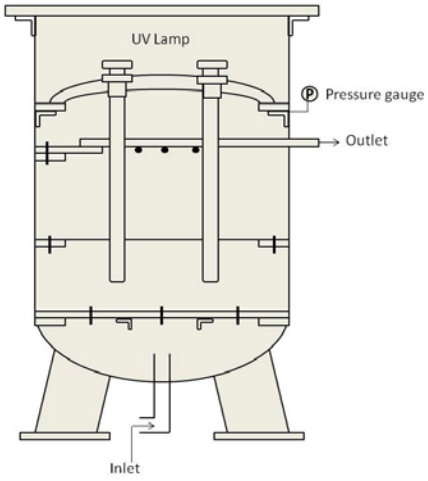

Figure 6:

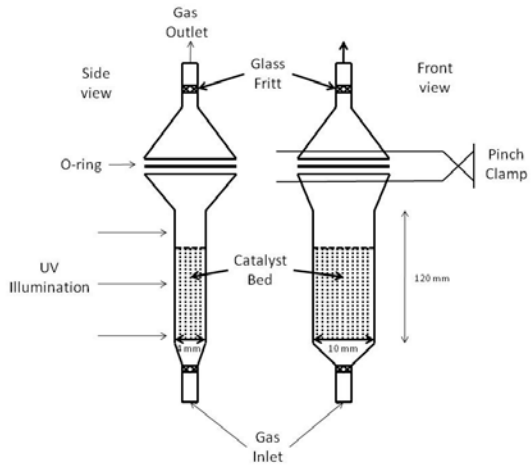

Figure 7:

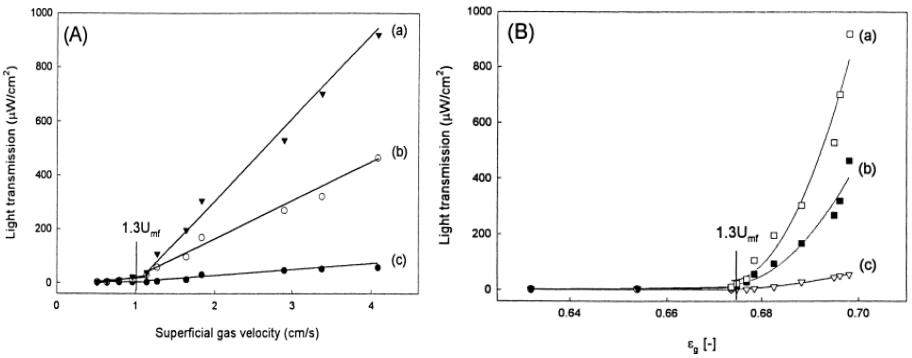

Figure 8:

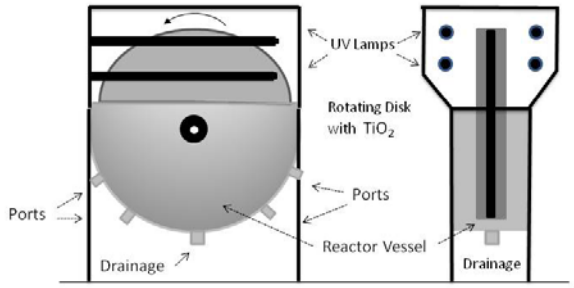

Figure 9:

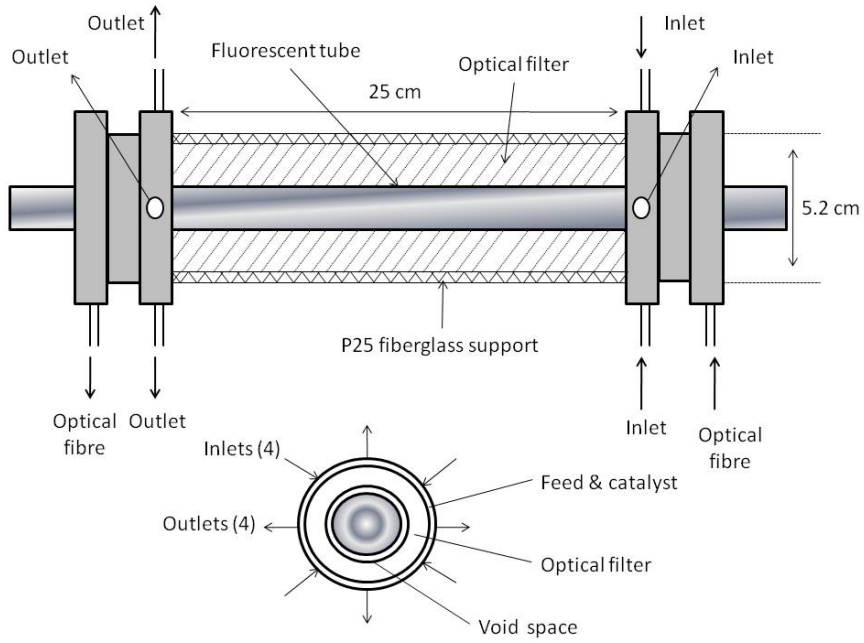

Figure 10:

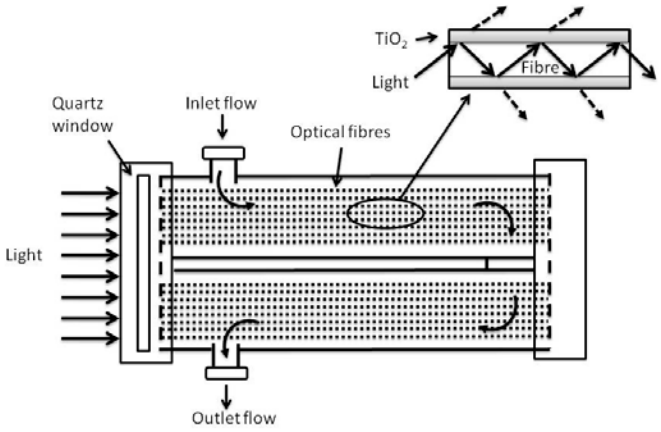

Figure 11:

(A)

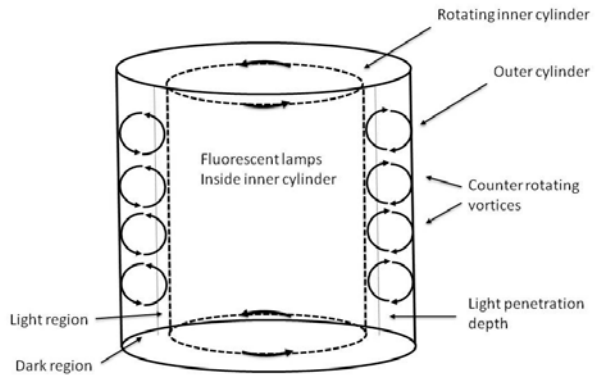

(B)

(C)

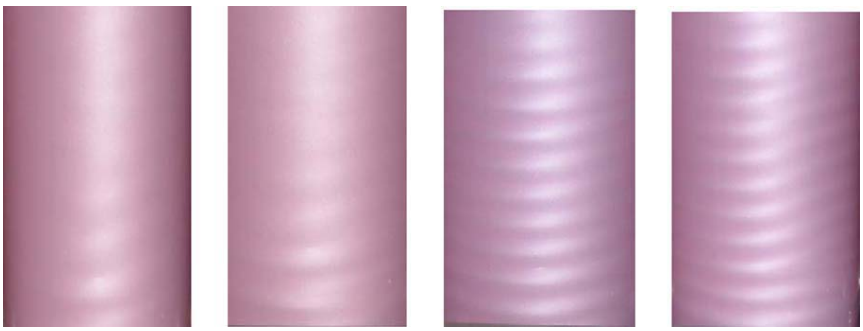

Figure 12:

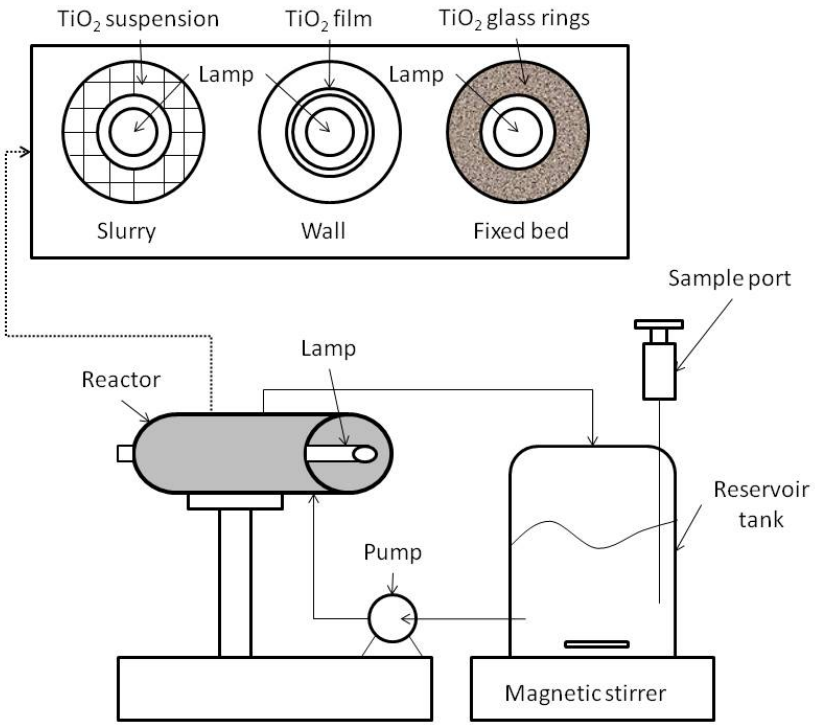

Figure 13:

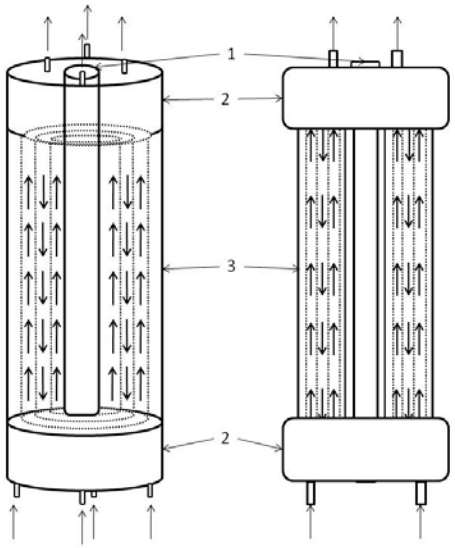

Figure 14:

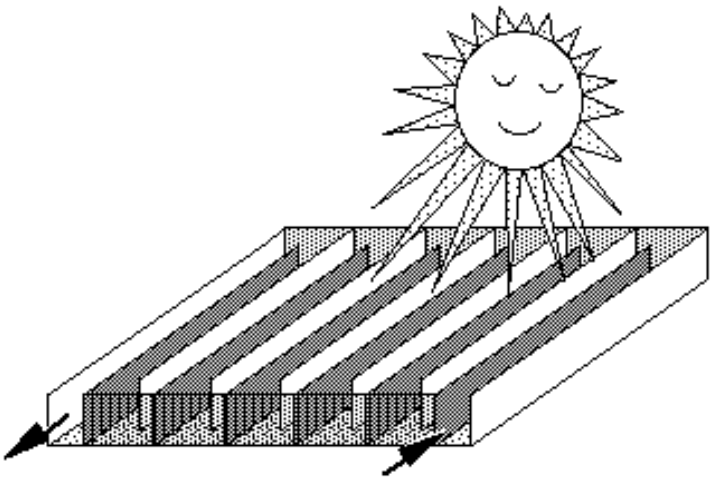

Captions for Figures

Figure 1: Page 5

Processes that occur on photo-excitation of TiO_2

Figure 2: Page 10

Chemical structure of the herbicides Monuron and 3,4-dichloropropionamide.

Figure 3: Page 11

Schematic of photocatalytic drum reactor

Figure 4: Page 13

(A) Temporal absorption spectral pattern displaying the degradation of MB over a 60 min time period and (B) effect of UV only, 30g catalyst (pellet form) only, UV combined with 30g catalyst and Degussa P25 (powder) effect on MB degradation.

Figure 5: Page 14

Schematic of fluidised bed reactor utilised for the destruction of microcystin-LR[33].

Figure 6: Page 15

Schematic of flat plate fluidised bed reactor displaying the illumination direction and catalyst bed location[66].

Figure 7: Page 16

Results observed for the effect of (A) superficial gas velocity and (B) voidage on light transmission with measuring light at (a) 96mm, (b) 53mm and (c) 10mm[75].

Figure 8: Page 23

Schematic representation of Rotating Disc Photo Reactor[80].

Figure 9: Page 27

Schematic representation (A) and sectional drawing (B) of the annular photoreactor[26].

Figure 10: Page 28

Schematic of Optical Fibre Photo Reactor displaying light transmission along coated fibres[92].

Figure 11: Page 30

(A) Schematic of taylor vortex reactor[29] and (B) Image of Taylor vortex photocataalytic reactor**.** (C) Progress of time-dependent Taylor vortex flow around critical Reynolds number, *Rec* = 111[28].

Figure 12: Page 32

(A) A slurry reactor, using suspensions of Degussa P25 TiO2. (B) A wall reactor, immobilizing Degussa P25 TiO2 onto the 15-cm long glass tube that constitutes the inner-tube wall of the reactor. (C) A fixed-bed reactor, immobilizing Degussa P25 TiO2 onto 6mm_ 6 mm glass Raschig rings placed into the annular reactor volume[96]

Figure 13: Page 33

Schematic representation of a pilot-scale multi-annular photocatalytic reactor, (A) UV lamp, (B) distribution heads, and (C) borosilicate glass tubes[100]

Figure 14: Page 35

Schematic View of a DSSR reactor[102] showing the inner structure of the transparent structured box made of PLEXIGLAS® (reproduced from xx with permission from Elsevier BV).